Clinical Cancer Research

Aberrant Thyroid-Stimulating Hormone Receptor Signaling Increases VEGF-A and CXCL8 Secretion of Thyroid Cancer Cells, Contributing to Angiogenesis and Tumor Growth

Young Shin Song[1,2], Min Joo Kim[1], Hyun Jin Sun[1], Hwan Hee Kim[1], Hyo Shik Shin[1], Young A. Kim[3], Byung-Chul Oh[4], Sun Wook Cho[1], and Young Joo Park[1,2]

Abstract

Purpose: Thyroid-stimulating hormone (TSH) suppression is widely used to treat well-differentiated thyroid cancer, whereas its role in poorly differentiated thyroid cancer (PDTC) is undetermined. Besides thyrocytes, TSH also binds to stromal cells, comprising tumor microenvironments. This study aimed to investigate the effects of TSH on tumor microenvironments in PDTC.

Experimental Design: An ectopic tumor model using PDTC cells (BHP10-3SCp and FRO), which exhibit TSH/cAMP-independent cell growth, was treated with TSH. IHC was performed using tissue microarrays from 13 PDTCs.

Results: TSH treatment significantly enhanced tumor growth of PDTCs with increased vascularity but not that of breast cancer cells, suggesting this effect is unique to thyroid cancer cells, not stromal cells. TSH significantly upregulated *VEGF-A* and *CXCL8* expressions in BHP10-3SCp cells via AKT and ERK signaling, resulting in higher concentrations of VEGF-A and CXCL8 in conditioned medium of TSH-treated BHP10-3SCp cells (TSH-CM) compared with controls. TSH-CM treatment enhanced tube formation potentials of endothelial cells, and blocking VEGF and/or CXCL8 reduced them. Blocking VEGF and/or CXCL8 also reduced TSH-dependent tumor growth with reduced tumor vasculature *in vivo*. TSH-treated tumors showed increased macrophage densities, and macrophage inhibition reduced TSH-dependent tumor growth *in vivo*. In human PDTCs, preoperative TSH levels were positively associated with VEGF-A and tumor size, and the expression of VEGF-A was positively correlated with CD31, CD163, and CXCL8, and their clinical poor prognosis.

Conclusions: Aberrant TSH receptor signaling modulates tumor angiogenesis by stimulating VEGF-A and CXCL8 secretion from PDTC cells and enhances tumor growth; thus, TSH suppression is beneficial for treating PDTCs.

Introduction

Thyroid cancer is the most common endocrine malignancy, and its incidence has robustly increased over the past 4 decades (1). Although most thyroid cancers are well-differentiated carcinomas, which are slow to progress and have an excellent prognosis, up to 30% of patients experience recurrence within 10 years (2, 3). To prevent recurrence, the long-term use of levothyroxine (T4) to suppress the endogenous pituitary excretion of thyroid-stimulating hormone (TSH), so-called T4 suppression therapy, has been generally considered for thyroid cancer patients at intermediate or high risk for recurrence (4–7).

TSH is a well-known growth factor for thyrocytes that leads to TSH-dependent growth of the thyroid gland, and higher serum TSH concentrations have been found to increase the oncogenic risk or tumor aggressiveness in well-differentiated thyroid cancer (WDTC; refs. 8–10). In contrast, the suppression of serum TSH concentration by administering levothyroxine was found to improve relapse-free and overall survival in high-risk patients with WDTC (11, 12), which supports the proposal that TSH suppression exerts inhibitory effects on the progression of WDTC. Thus, T4 suppression therapy has long been used as an essential therapeutic strategy for the treatment of WDTC, especially in high-risk cases (4–7).

However, T4 suppression therapy should be considered after weighing the potential risks and benefits of TSH suppression (4–7), because long-term, aggressive suppression of TSH could be related to systemic adverse events, such as the exacerbation of ischemic heart disease, as well as an increased risk of atrial fibrillation (13) and osteoporosis (14, 15). The molecular characteristics of WDTC cells have been found to undergo alterations during disease progression; the loss of the TSH receptor (TSHR) and/or sodium/iodide symporter (NIS) is often observed in

[1]Department of Internal Medicine, Seoul National University Hospital, Seoul, Republic of Korea. [2]Department of Internal Medicine, Seoul National University College of Medicine, Seoul, Republic of Korea. [3]Department of Pathology, Seoul Metropolitan Government - Seoul National University Boramae Medical Center, Seoul, Republic of Korea. [4]Lee Gil Ya Cancer and Diabetes Institute, Gachon University Graduate School of Medicine, Incheon, Republic of Korea.

Note: Supplementary data for this article are available at Clinical Cancer Research Online (http://clincancerres.aacrjournals.org/).

Corresponding Authors: Young Joo Park, Seoul National University College of Medicine, 103 Daehak-ro, Jongno-gu, Seoul 03080, Republic of Korea. Phone: 82-2-2072-4183; Fax: 82-2-762-2292; E-mail: yjparkmd@snu.ac.kr; and Sun Wook Cho, Department of Internal Medicine, Seoul National University Hospital, 101 Daehak-ro, Jongno-gu, Seoul 03080, Republic of Korea. Phone: 82-2-2072-4761; Fax: 82-2-762-2292; E-mail: swchomd@snu.ac.kr

doi: 10.1158/1078-0432.CCR-18-0663

Translational Relevance

This study demonstrated that thyroid-stimulating hormone (TSH) stimulated the production of angiogenic factors in thyroid cancer cells, which showed TSH/cAMP-independent cell growth, through aberrant TSH/AKT and ERK signaling. Consequently, TSH-stimulated tumor angiogenesis contributed to tumor growth in association with increasing macrophage recruitment *in vivo*. In human poorly differentiated thyroid cancers (PDTCs), TSH levels were positively associated with VEGF-A and tumor size, and the expression of VEGF-A was positively correlated with CD31, CD163, and CXCL8, as well as their clinical poor prognosis. Taken together, the present study supports the usefulness of TSH suppression by T4 suppression therapy, even in PDTC. In addition, these proangiogenic effects of TSH were minimal and did not enhance tumor growth in an ectopic tumor model of breast cancer, indicating that the direct effects of TSH on endothelial cells were negligible in human cancers other than thyroid.

poorly differentiated thyroid cancers (PDTC; ref. 16). Subsequently, these changes attenuate the iodine uptake potential, resulting in iodine-refractory incurable diseases. In *in vitro* experiments, the response to TSH stimulation measured in terms of cAMP levels (17) or iodine uptake (18) was also markedly decreased in some thyroid cancer cell lines, and these cancer cells often showed TSH-independent tumor growth (19). Therefore, it is reasonable to deduce that the role of T4 suppression therapy might be negligible in this setting.

Meanwhile, several pieces of evidence have shown that TSH not only regulates tumor cell growth, but also simulates cytokine production in tumor cells, which could affect the tumor microenvironment (19–21). These findings led us to hypothesize that TSH would influence the tumor microenvironment via the paracrine secretions of tumor cells, which could potentially be associated with T4 suppression therapy having advantages not limited to the suppression of TSH-dependent cell growth. Moreover, TSH also binds to extrathyroidal cells including fibroblast or endothelial cells (22, 23), which are essential members of tumor stroma, and may have potential for directly modulating tumor microenvironments. The aim of this study was to investigate the role of TSH on the tumor microenvironment and its effects on tumor growth and progression.

Materials and Methods

Study design

To identify the effects of TSH on tumor growth and angiogenesis, the ectopic tumor models using PDTC cells harboring *TSHR* or a breast cancer cell line which did not express *TSHR* were treated with TSH. To obtain a mechanistic insight, proangiogenic effects of conditioned medium (CM) of TSH-treated PDTC cells were studied using human microvascular endothelial cells. Angiogenic factors were screened using cytokine array, and VEGF-A and CXCL8 were increased. To explore whether these factors mediated TSH effects on PDTC tumor angiogenesis, neutralizing antibodies were administered to TSH-treated ectopic tumors *in vivo*. Finally, clinical relevance was studied in PDTC tumor microarray with IHC.

Reagents

Recombinant human TSH (rhTSH; Thyrogen) from Genzyme Therapeutics, MMI from Sigma-Aldrich, bevacizumab (anti-VEGF; Avastin) from Roche, and clodronate liposomes from FormuMax Scientific Inc. were used. Anti–VEGF-A antibody, anti-CXCL8 antibody, and ELISA kits for VEGF-A and CXCL8 were purchased from R&D Systems. The inter- and intra-assay coefficients of variation were 4.1% and 6.7% for VEGF-A and 4.6% and 6.7% for CXCL8. The linear ranges of VEGF-A (27 kDa) and CXCL8 (11 kDa) were 7.8 to 1,000 pg/mL and 15.6 to 2,000 pg/mL, respectively.

Cell culture and CM

To investigate effects of TSH in PDTC, two PDTC cell lines, BHP10-3SCp and FRO cells, were used. The BHP10-3SCp cell line was established as a tumorigenic subclone of BHP10-3 cells, a human papillary thyroid cancer (PTC) cell line harboring the RET/PTC rearrangement that was kindly provided by Dr. Soon-Hyun Ahn (Seoul National University College of Medicine, Seoul, Republic of Korea) and Dr. Gary L. Clayman (MD Anderson Cancer Center, Houston, TX; ref. 24). The original BHP10-3 cell line was authenticated by the short tandem repeat typing method in April 2015 and verified again after being established as a tumorigenic subclone in July 2015. The last authentication was performed in June 2016. The FRO cell line and two PTC cell lines, TPC-1 and BCPAP, were kindly provided by Dr. June-Key Chung (Seoul National University College of Medicine, Seoul, Republic of Korea). A human triple-negative breast cancer cell line MDA-MB-231, a kind gift from Dr. Hyo Soo Kim (Seoul National University College of Medicine, Seoul, Republic of Korea), was used to distinguish the direct effects of TSH on thyroid cancer cells and the surrounding endothelial cells.

BHP10-3SCp cells were seeded on 100-mm culture dishes with 3×10^5 cells/mL with complete RPMI-1640 medium containing 10% FBS. When cells reached a >90% confluent monolayer, 20 ng/μL of rhTSH or saline was administered in serum-free medium. After 24 hours, the CM was harvested from each cell culture, filtered, and stored at −70°C. CMs from rhTSH-treated BHP10-SCp cells were referred to as TSH-CM/B, and saline-treated CMs from BHP10-SCp cells were referred to as control-CM/B. An angiogenesis antibody array (R&D Systems) was used to test the protein expression of angiogenic cytokines in TSH-CM/B.

Animal experiments

Five-week-old female BALB/c nu/nu mice were purchased from Orient Bio Inc. and housed in a dedicated pathogen-free facility. The Institutional Animal Care and Use Committee of Seoul National University approved the protocols for the animal study (no. SNU-141224-2). All animals were maintained and used in accordance with the Guidelines for the Care and Use of Laboratory Animals of the Institute of Laboratory Animal Resources, Seoul National University.

BHP10-3SCp (5×10^6/50 μL of PBS), FRO (2×10^6/50 μL of PBS), or MDA-MB-231 (2×10^6/50 μL of PBS) cells were mixed with 50 μL of Matrigel (BD Biosciences) and implanted subcutaneously in the flank area of each mouse. Five days after tumor cell injection, when visible tumors began to appear, rhTSH was started to administer intraperitoneally (5 days/week) until day 28, and saline (0.9% NaCl) was used for the controls ($n = 8$ in each group). In the BHP-10-3SCp tumor mouse model, to determine the dose-dependent effect of TSH, rhTSH were administered at

two different doses of 0.15 μg/g (low-TSH) and 1.5 μg/g (high-TSH), which were considered to lead to the physiologic and supraphysiologic responses in mouse (25). Because the high-TSH group showed more obvious difference from the control than the low-TSH group in the BHP-10-3Sp tumor model, in the FRO and MDA-MB-231 models, high doses (1.5 μg/g) of rhTSH were used. Tumor size was measured at least twice per week, and tumor volume was calculated using the following equation: volume $= {}^1/_2 \times a \times b^2$, where $a =$ the long tumor diameter and $b =$ the short tumor diameter (26). On day 28, all mice were euthanized, and blood was collected 24 hours after the last injection of rhTSH or saline. For experiments involving treatment with MMI, MMI was dissolved in water (0.025%) and applied to mice from day 7 to day 28 after tumor cell injection. Tap water was used in the controls ($n = 8$ in each group).

In the BHP10-3SCp tumor mouse model, to confirm the effects of VEGF-A and CXCL8 induced by TSH, anti-VEGF (1 μg/g, 3 days/week) and anti-CXCL8 (50 μg/g, once a week) were i.p. injected in the TSH group (high-TSH; $n = 8$ in each group). For the *in vivo* macrophage depletion study, clodronate liposomes (35 μg/g, 2 days/week) or control liposomes were i.p. injected in both the control and TSH groups ($n = 8$ in each group). All animal experiments were performed at least twice independently.

Measurement of serum TSH and free T4

Serum murine TSH levels were measured using a TSH ELISA kit (MPTMAG-49K, Millipore) according to the manufacturer's instructions. Serum-free T4 and human TSH levels were measured using an immunoradiometric assay kit (IRMA, Shin Jin Medics Inc.) following the manufacturer's instructions. Serum TSH and free T4 levels were measured in mouse serum samples obtained 24 hours after the last injection of rhTSH.

IHC staining of tumors from animal models

The tumors from xenograft models were fixed in 4% paraformaldehyde and embedded in paraffin. IHC staining was performed using anti-mouse CD31 (1:100, Santa Cruz Biotechnology), ERG (predilute, *Ventana* Medical Systems), VEGF-R2 (1:100, Cell Signaling Technology), F4/80 (1:200, eBioscience), and anti-human Ki-67 (1:500, Neomarkers).

Transwell migration assay and tube formation assay

Human microvascular endothelial cells (HMVEC), purchased from Lonza, were cultured in 0.5% BSA/EBM-2 medium (Lonza) and used for assays. More details are in Supplementary Materials and Methods.

Western blot analysis

BHP10-3SCp cells were treated with rhTSH (20 ng/μL), and the cell lysates were harvested at 0, 15, 30, and 120 minutes. The primary antibodies were pAKT (1:2,000, #4058), AKT (1:2,000, #9272), pERK (1:2,000, #4370), and ERK (1:2,000, #9102) from Cell Signaling Technology, and β-ACTIN (A5441) from Sigma-Aldrich. More details are in Supplementary Materials and Methods.

RT-PCR

After 6 hours of starvation, BHP10-3SCp cells were pretreated with TSH receptor antibody or inhibitors of PI3K/mTOR and ERK at 2 hours after rhTSH administration (20 ng/μL). K1-70 (100 ng/μL, RSR Ltd.) was used as a TSH receptor blocking antibody. LY294002, RAD001, and PD98059 (10 μmol/L for all, Sigma-Aldrich) were used to inhibit PI3K, mTOR, and ERK activity, respectively. Seventy-two hours after the treatment, the cells were washed, and the mRNA was harvested with Trizol (Invitrogen). RT-PCR was done using an ABI Prism 7500 Sequence Detection System (Applied Biosystems). The sequences of the primers are listed in Supplementary Table S1.

Human tissue microarray and IHC staining

Paraffin-embedded PDTC samples from 13 patients and advanced PTC samples defined as ≥2 cm-sized tumors from 35 patients were used for constructing tissue microarray as previously described (27). IHC staining of the tissue microarrays was performed using anti-human VEGF-A (1:30, R&D systems), CXCL8 (1:500, Novus Biologicals), CD31 (1:1,000, Cell Signaling Technology), ERG (predilute, *Ventana* Medical Systems), and CD163 (1:1,000, Cell Signaling Technology). All images were analyzed using the publicly available programs Image J (28), Immunoratio (29), and ImageScope (Aperio). All experiments were approved by the Institutional Review Board of Seoul National University Hospital (1107-060-369).

Statistical analysis

For statistical comparisons, the Mann–Whitney test or the two-tailed Student *t* test was used for two groups, and the Kruskal–Wallis test with the Bonferroni correction was used for three groups. Comparisons of categorical variables were performed with either Pearson χ^2 test or Fisher exact test. Relationships between each IHC marker in human PDTC samples were evaluated by the Pearson correlation coefficient. Statistical significance was defined as two-sided P values < 0.05.

Results

TSH enhanced tumor growth and angiogenesis in thyroid cancer

To investigate the effects of TSH on tumor growth, BHP10-3SCp cells, a tumorigenic subclone of BHP10-3M cells originating from a PTC patient, were used. BHP10-3SCp cells did not show TSH-dependent cell growth (Supplementary Fig. S1A) or cAMP production (Supplementary Fig. S1B) in comparison with the normal rat thyrocytes, FRTL-5 cells. Thyroid differentiation–related genes such as *thyroid transcription factor-1*(*TTF-1*), *TSHR*, and *paired-box gene 8* (*PAX8*) were rarely detected in BHP10-3SCp cells (Supplementary Fig. S2A), suggesting poorly differentiated status of it. Meanwhile, *PAX8*, not *TTF1* nor *TSHR*, was upregulated in response to the 72-hour treatment of rhTSH (Supplementary Fig. S2B). Therefore, it is reasonable to deduce that BHP10-3SCp is a PDTC cell line dedifferentiated from a DTC cell line, as previously reported (30).

Next, BHP10-3SCp cells were transplanted into athymic nude mice to establish an ectopic tumor model, and rhTSH at two different doses (0.15 μg/g for low-TSH group; 1.5 μg/g for high-TSH group), or saline was administered intraperitoneally from day 5 to day 28. On day 10, the tumor volume of high-TSH group was larger than that of the control group, whereas there was no significant difference between low-TSH group and control group (Fig. 1A). On day 14, the tumor volumes of the low-TSH and high-TSH groups versus the controls were significantly different, by 1.9-fold ($P = 0.021$) and 2.7-fold ($P = 0.043$), respectively (Fig. 1A). The tumors in the low-TSH and high-TSH groups were

approximately 2.3-fold larger at day 21 and 2.5-fold larger at day 28 than those of the controls ($P < 0.05$ and $P < 0.001$ at day 21, respectively; $P < 0.05$ and $P < 0.01$ at day 28, respectively). Tumor volume was not statistically significantly different between the low-TSH and high-TSH groups on day 21 or 28 (Fig. 1A). Human TSH levels measured in mouse serum were highest in the high-TSH group, followed by the low-TSH group, whereas the levels in the controls were undetectable (Fig. 1B). Free T4 levels were

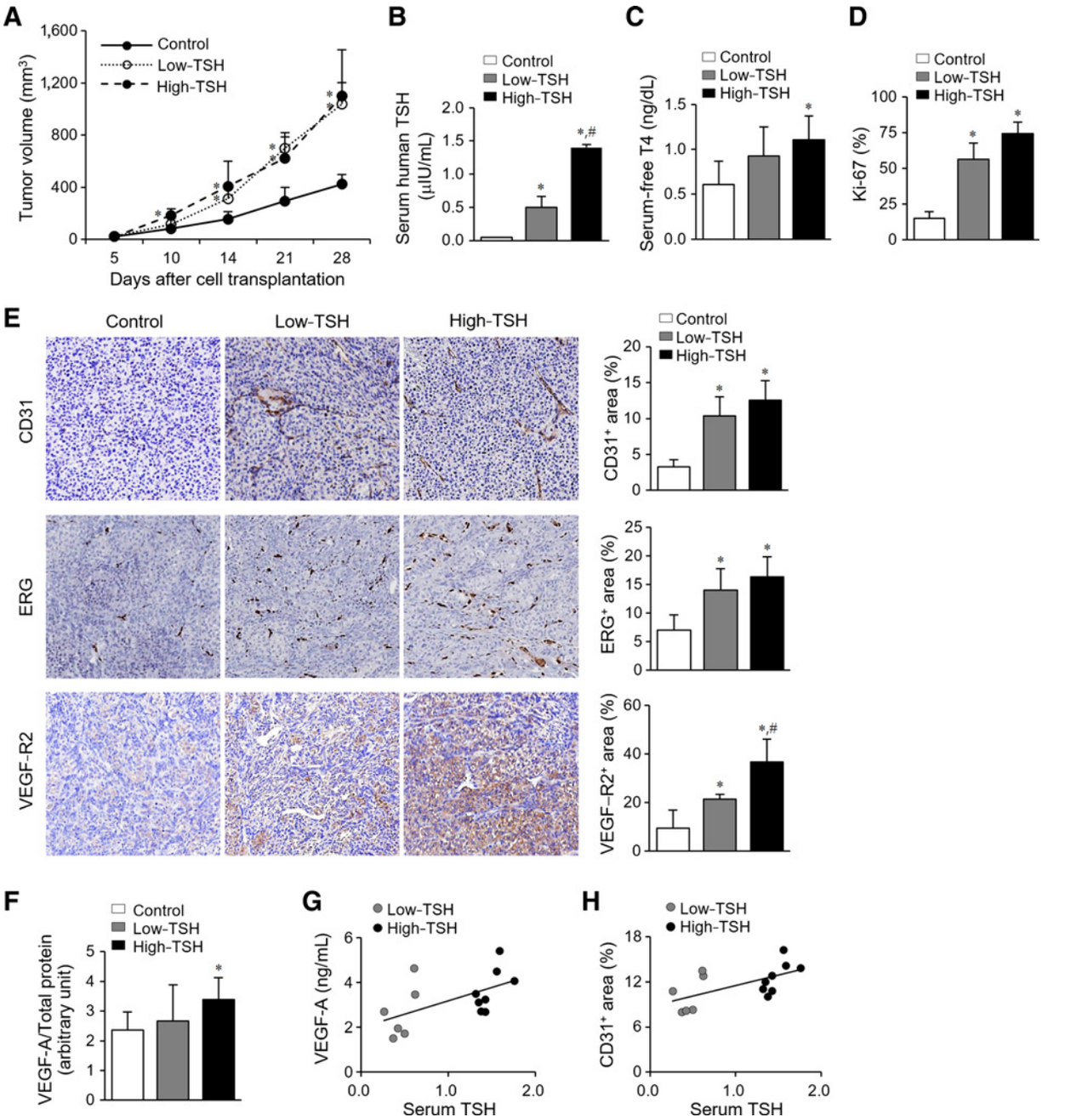

Figure 1.

Effects of TSH treatment on tumor growth and angiogenesis in PDTC. BHP10-3SCp cells were s.c. injected into nude mice (5 weeks old), and recombinant human TSH (0.15 μg/g in the low-TSH group; 1.5 μg/g for the high-TSH group) or saline was administered intraperitoneally from day 5 to day 28 ($n = 8$ in each group). **A,** Tumor growth in each group was monitored by measuring tumor volume during the treatment period. *, $P < 0.05$ versus controls. On day 28, (**B**) human TSH and (**C**) murine free T_4 levels were measured in mouse serum samples obtained 24 hours after the last injection of rhTSH. *, $P < 0.05$ versus controls; #, $P < 0.05$ versus low-TSH. IHC staining for (**D**) Ki-67 (a graph of its density) and (**E**) CD31, ERG, and VEGF-R2 was done in tumor tissues (×200). *, $P < 0.05$ versus controls; #, $P < 0.05$ versus low-TSH. **F,** VEGF-A levels were measured in tumor lysates using an ELISA assay. *, $P < 0.05$ versus controls. All data are expressed as mean ± SD. Correlations of serum human TSH levels with (**G**) VEGF-A levels analyzed by ELISA and (**H**) $CD31^+$ area of IHC.

significantly higher in the high-TSH group than in controls, whereas no difference was found between the low-TSH and control groups (Fig. 1C). The density of Ki-67 staining, a marker of proliferation, was higher in the low-TSH and high-TSH groups than in the controls (Fig. 1D).

Because TSH had a minimal direct effect on the viability of BHP10-3SCp cells (Supplementary Fig. S1), we then hypothesized that the positive effects of TSH on PDTC tumor growth *in vivo* were due to its effects on the tumor microenvironment. Interestingly, IHC staining using anti-CD31 and anti-ERG demonstrated that tumors from the low-TSH and high-TSH groups showed a higher vascular density than those from controls (Fig. 1E). IHC staining (Fig. 1E) and Western blot analyses (Supplementary Fig. S3) showed that VEGF-R2 was highly expressed in the low-TSH and high-TSH groups compared with the controls. An ELISA assay of tumor lysates showed that VEGF-A expression likewise increased in the high-TSH group by 1.4-fold in comparison with the controls (Fig. 1F), and it was positively correlated with the serum TSH levels with marginal significance ($r = 0.532$, $P = 0.075$, Fig. 1G). Furthermore, the serum TSH levels showed positive correlation with $CD31^+$ area of IHC, significantly ($r = 0.594$, $P = 0.042$, Fig. 1H).

For validation, the effects of TSH on tumor growth and angiogenesis were further evaluated in the mouse tumor model using FRO cells. Similar to BHP10-3SCp cells, TSH enhanced tumor growth (Supplementary Fig. S4A) and vascularity measured by the immunoreactivity score of CD31-positive cells (Supplementary Fig. S4B). Collectively, TSH treatment enhanced tumor growth in association with augmented tumor angiogenesis.

TSH enhanced tumor growth and angiogenesis independently of thyroid hormone

Because TSH stimulates thyroid hormone production, these effects of exogenous rhTSH might have resulted from the actions of both TSH and thyroid hormone. Although free T4 levels in the low-TSH group were not significantly higher than in the controls and resulted in as large of an increase in tumor growth as was observed in the high-TSH group, the effects of thyroid hormone were still possibly present. To exclude the effects of thyroid hormone from those of elevated TSH, an MMI-induced hypothyroidism model, which exhibits high TSH but low thyroid hormone, was used. BHP10-3SCp cells were s.c. injected to nude mice and MMI (0.025%) or tap water was administered by drinking water from day 7 to day 28. After 4 weeks, the tumor volume in the MMI group was larger than in the controls by 1.7-fold ($P = 0.010$), although the size was smaller than in the high-TSH or low-TSH groups (Supplementary Fig. S5A). Serum mouse TSH was higher (714.7 ± 342.7 pg/mL vs. 181.8 ± 55.3 pg/mL, $P = 0.025$, Supplementary Fig. S5B), and serum-free T4 was lower (0.52 ± 0.47 ng/dL vs. 1.11 ± 0.41 ng/dL, $P = 0.038$, Supplementary Fig. S5C) in the MMI group than in the control group. In the IHC staining of tumor tissues, positivity for CD31 (Supplementary Fig. S5D) and Ki-67 (Supplementary Fig. S5E) was significantly higher in the MMI group than in the controls. Moreover, the tumor lysates showed higher VEGF-A levels in the MMI group than in the controls (Supplementary Fig. S5F), suggesting that similar angiogenic changes were induced in this model to those found in the TSH injection model. Taken together, TSH enhanced tumor growth and angiogenesis independently of thyroid hormone in BHP10-3SCp PDTC tumor models.

TSH enhanced tumor angiogenesis not by directly affecting endothelial cells, but by stimulating secretions of VEGF-A and CXCL8 from thyroid cancer cells

Because a recent study showed that TSH stimulated angiogenic potentials in human endothelial cells (22), we hypothesized that TSH might directly affect endothelial cells in thyroid cancer microenvironments. To test this hypothesis, we used a triple-negative breast cancer cell line, MDA-MB-231, which showed extremely lower expression of *TSHR* in RT-PCR analysis (Supplementary Fig. S6A). Treatment of rhTSH did not change transcriptions of *VEGF-A* or *CXCL8* (Supplementary Fig. S6B). Cells were transplanted in athymic nude mice, and rhTSH was injected from 1 to 4 weeks. Four weeks after cell transplantation, the tumor volumes of the TSH group showed no statistically significant difference compared with those of the control group (Supplementary Fig. S6C), although serum human TSH levels were significantly higher in the TSH group (Supplementary Fig. S6D).

Next, we hypothesized that treatment of thyroid cancer cells with TSH may lead to the creation of a proangiogenic environment. To test this hypothesis, the CM of TSH-treated BHP10-3SCp cells was harvested and administered to HMVECs. First, a cell viability assay was performed using a CCK-8 assay, and TSH-CM/B showed significantly increased cell viability at 24 hours in HMVECs by 1.3-fold (Fig. 2A). Treatment with TSH-CM/B significantly increased the cell migration potential of HMVECs in a transwell assay compared with the control-CM/B (Fig. 2B). Moreover, the tube formation potential was also enhanced in the TSH-CM/B treatment group in comparison with the control-CM/B group (Fig. 2C). To explore the TSH-mediated secretory factors that augmented the angiogenic potential of human vascular endothelial cells, TSH-CM/B was analyzed using a cytokine array containing 56 angiogenesis-related proteins. Among them, VEGF-A and CXCL8 expression showed the greatest increases in expression in the TSH-CM/B group compared with the control-CM/B group. An ELISA assay showed that VEGF-A (11.84 ± 0.59 ng/mL vs. 5.66 ± 0.28 ng/mL, $P < 0.01$, Fig. 2D) and CXCL8 (3.84 ± 0.47 ng/mL vs. 2.81 ± 0.33 ng/mL, $P < 0.01$, Fig. 2E) showed significant increases in the TSH-CM/B group compared with the control-CM/B group.

TSH stimulated VEGF-A and CXCL8 secretion via AKT/mTOR and ERK signaling in thyroid cancer cells

To obtain insights into the molecular mechanism of the effects of TSH on VEGF-A and CXCL8 production in BHP10-3SCp cells, AKT and ERK phosphorylation, which are known to be activated via a TSH receptor–activated PKC pathway, were evaluated (31). Because TSH did not increase cAMP production or cell growth in BHP10-3SCp cells (Supplementary Fig. S1), we then hypothesized that TSH influenced cytokine production via the PKC pathway. Interestingly, treatment with TSH stimulated the phosphorylation of AKT and ERK (Fig. 2F). Furthermore, TSH-mediated *VEGF-A* and *CXCL8* expressions were significantly blocked by TSH receptor blocking antibody (K1-70) and inhibitors of PI3K (LY294002), mTOR (RAD001), and ERK (PD98059; Fig. 2G and H), indicating that TSH increased VEGF-A and CXCL8 secretion via PI3K/AKT/mTOR or ERK signaling in BHP10-3SCp cells.

Blocking VEGF-A and/or CXCL8 inhibited TSH-mediated tumor angiogenesis and tumor growth

To inhibit the effects of TSH-stimulated VEGF-A and/or CXCL8, neutralizing antibodies for each molecule were treated

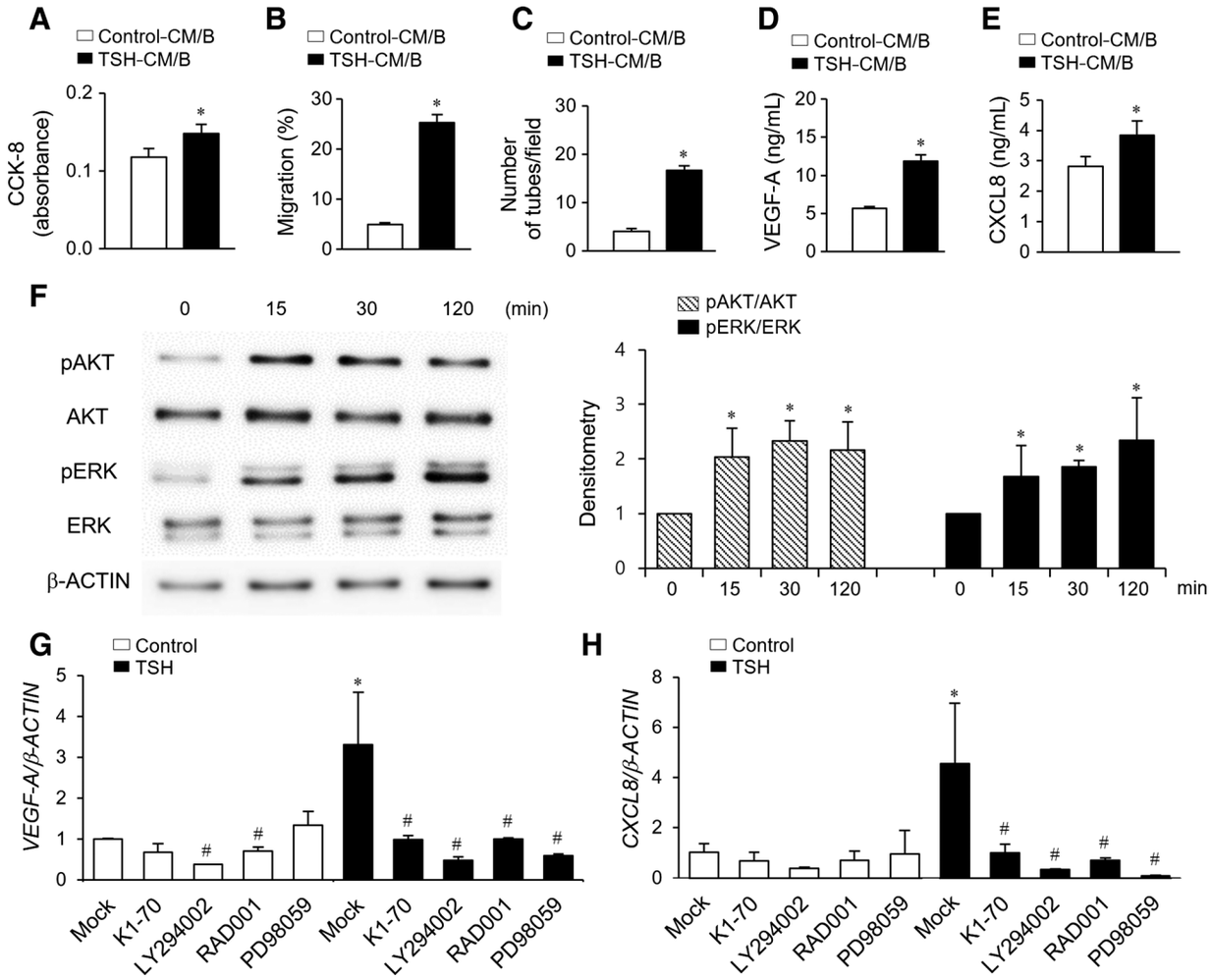

Figure 2.

Angiogenic effects of TSH by stimulating secretion of VEGF-A and CXCL8 from PDTC cells via AKT/mTOR and ERK signaling. **A–H,** BHP10-3SCp cells were treated with TSH (20 ng/μL) or saline for 24 hours, and CM was harvested (TSH-CM/B and control-CM/B) and administered to HMVEC. **A,** After 24 hours of TSH-CM/B or control-CM/B treatment, a CCK-8 assay was performed to test cell viability. **B,** HMVECs were plated for a transwell migration assay and treated with TSH-CM/B or control-CM/B. After 4 hours, the migrated cells were stained and quantified using Image J. *, $P < 0.05$ versus control-CM/B. **C,** The HMVECs were cultured with EBM-2 medium containing TSH-CM/B or control-CM/B. The number of tubes per field was measured in 3 randomly selected fields (×100). *, $P < 0.05$ versus control-CM/B. (**D**) VEGF-A and (**E**) CXCL8 concentrations were measured in TSH-CM/B and control-CM/B using an ELISA assay. *, $P < 0.05$ versus control-CM/B. **F,** BHP10-3SCp cells were treated with TSH (20 ng/μL), and proteins were harvested from total cell lysates 0, 15, 30, and 120 minutes after treatment. Western blot analysis was performed with anti-pAKT, anti-AKT, anti-pERK, and anti-ERK. *, $P < 0.05$ versus 0 minutes. **G** and **H,** BHP10-3SCp cells were pretreated with TSH receptor blocking antibody (K1-70), a PI3K inhibitor (LY294002), an mTOR inhibitor (RAD001), or an ERK inhibitor (PD98059) for 2 hours, following TSH (20 ng/μL) treatment. After 72 hours, mRNA was harvested, and (**G**) *VEGF-A* and (**H**) *CXCL8* expressions were analyzed by real-time RT-PCR. *, $P < 0.05$ versus mock in controls; #, $P < 0.05$ versus mock in each group. All data are expressed as mean ± SD.

respectively and/or coincidently. Transwell migration and tube formation potentials of TSH-CM/B–treated HMVECs were evaluated after treatment of anti-CXCL8 or anti-VEGF-A, or both. Treatment with the neutralizing antibody of CXCL8 inhibited the TSH-CM/B–mediated increases of cell migration potential (Fig. 3A and B), but did not inhibit TSH-CM/B–dependent tube formation (Fig. 3A and C). Meanwhile, treatment with the neutralizing antibody of VEGF-A blocked TSH-CM/B–mediated increases in cell migration and tube formation potential in HMVECs (Fig. 3A–C). Moreover, blocking VEGF-A and CXCL8 coincidently showed further inhibition of tube formation potential compared with what was observed when blocking VEGF-A alone (Fig. 3A–C). In *in vivo* experiments, nude mice injected with BHP10-3SCp cells subcutaneously were divided into five groups: control, TSH, TSH + anti-VEGF-A, TSH + anti-CXCL8, and TSH + anti-VEGF-A + anti-CXCL8. TSH increased tumor volume by 1.4-fold compared with the control. Conversely, tumor volume was significantly decreased by blocking VEGF-A, CXCL8, and both compared with the TSH group (volume reduction of 34%, 54%, and 60% at day 28, respectively; Fig. 3D). IHC staining of the tumors revealed that the ERG expression in vascular endothelial cells of tumors was increased by TSH treatment, whereas the TSH effect was diminished by treatment of anti–VEGF-A, anti-CXCL8, or both (Fig. 3E).

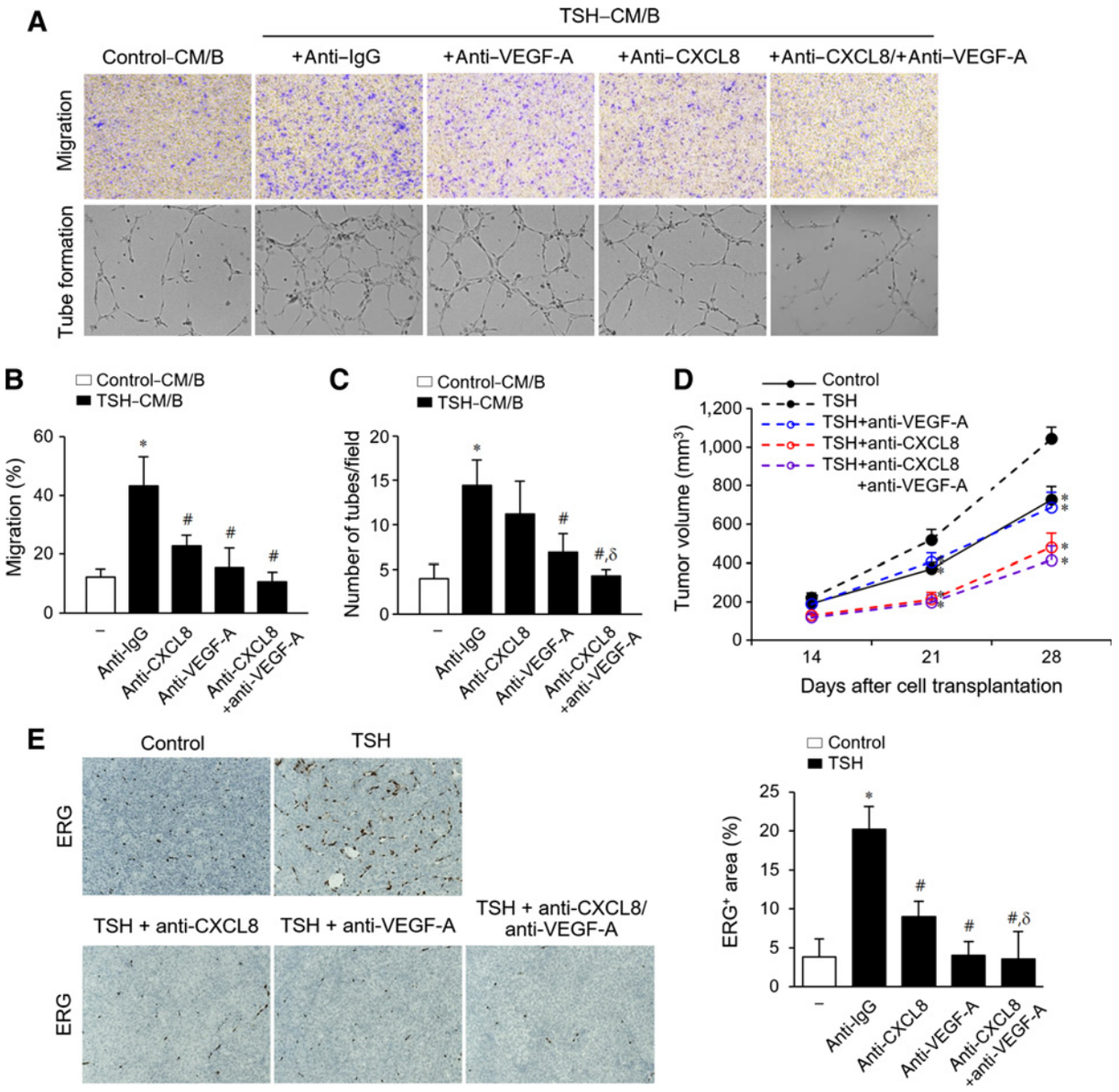

Figure 3.

Blocking VEGF-A and/or CXCL8 inhibited TSH-induced tumor angiogenesis and tumor growth. **A–C,** Transwell migration and tube formation potentials of TSH-CM/B–treated HMVECs were evaluated after treatment of anti-CXCL8 (10 μg/mL) or anti–VEGF-A (10 μg/mL), or both. **A,** Representative images of transwell migration assay (top) and tube formation assay (bottom) of each group. **B,** Migrated cells were stained and quantified using Image J. **C,** The number of tubes per field was measured in 3 randomly selected fields (×100). *, $P < 0.05$ versus control-CM/B; #, $P < 0.05$ versus TSH-CM/B with anti-IgG; δ, $P < 0.05$ versus TSH-CM/B with anti–VEGF-A. **D** and **E,** Nude mice injected with BHP10-3SCp cells subcutaneously were divided into 5 groups and administered as follows: saline (control), recombinant human TSH (TSH), TSH + anti–VEGF-A, TSH + anti-CXCL8, TSH + anti-CXCL8 + anti–VEGF-A, respectively ($n = 8$ in each group). **D,** Tumor growth in each group was monitored by measuring tumor volume during the treatment period. *, $P < 0.05$ versus TSH. **E,** IHC staining for ERG was done in tumor tissues (×200). *, $P < 0.05$ versus controls; #, $P < 0.05$ versus TSH; and δ, $P < 0.05$ versus anti-CXCL8. All data are expressed as mean ± SD.

TSH-enhanced tumor vasculatures were associated with increased macrophage recruitment and tumor growth

To explore the biological impact of TSH-induced angiogenesis in the tumor microenvironment, we evaluated macrophage densities in tumors of the mouse model with BHP10-3SCp cells, because tumor-associated macrophages have been shown to support tumor progression in thyroid cancers (32). IHC staining with F4/80 demonstrated that a high density of macrophages was observed in the high-TSH group compared with the controls, especially in the perivascular area (Fig. 4A). Transwell migration assays using human monocyte/macrophage (THP-1) cells demonstrated that treatment of TSH did not enhance cell migration potentials in THP-1 alone (Supplementary Fig. S7A) or in coculture with BHP10-3SCp cells (Supplementary Fig. S7B), suggesting

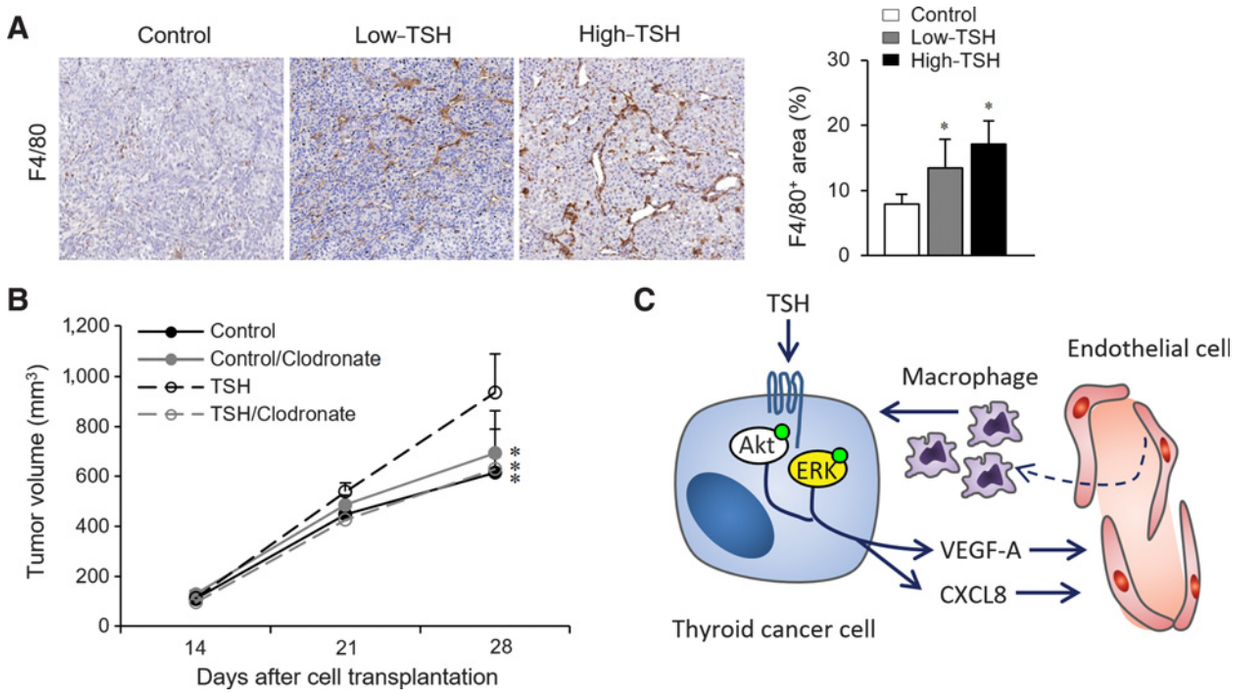

Figure 4.

Effects of TSH on macrophage recruitment and the microenvironment of PDTC. **A** and **B,** BHP10-3SCp cells were s.c. injected into nude mice, and recombinant human TSH or saline was administered intraperitoneally from day 5 to day 28 ($n = 8$ in each group). **A,** IHC staining using anti-F4/80 antibody was done in tumor tissues (×100). *, $P < 0.05$ versus controls. **B,** Recombinant human TSH or saline was administered with or without clodronate, and tumor growth in each group was monitored by measuring tumor volume during the treatment period. *, $P < 0.05$ versus TSH. All data are expressed as mean ± SD. **C,** Working model. TSH receptor signaling activated aberrant signaling, such as the AKT and ERK pathways, and increased VEGF-A and CXCL8 production in thyroid cancer cells. Secreted VEGF-A and CXCL8 affected endothelial cells in the tumor vasculature and subsequently increased macrophage recruitment, which enhanced tumor growth of thyroid cancer.

that the recruitment of macrophages was increased via enhanced vasculature rather than the direct chemotactic effects of TSH. Finally, in *in vivo* model, when rhTSH or saline was administered with or without clodronate-liposome, a macrophage inhibitor, treatment of clodronate-liposome reduced TSH-dependent tumor growth (Fig. 4B). Thus, TSH-enhanced tumor angiogenesis resulted in tumor growth by increasing tumor-associated macrophage recruitment into the tumor microenvironment.

Taken together, TSH stimulated VEGF-A and CXCL8 secretion from thyroid cancer cells via the AKT/mTOR and ERK signaling pathways. Secreted VEGF-A and CXCL8 affected endothelial cells in the tumor vasculature and subsequently increased macrophage recruitment, which enhanced tumor growth of thyroid cancer (Fig. 4C).

Associations between preoperative serum TSH, angiogenic factors, and macrophage density in human PDTCs

To validate the clinical relevance of VEGF-A and CXCL8 expression in human PDTC, we performed IHC staining of VEGF-A, CXCL8, CD31, ERG, and a macrophage marker, CD163, on human tissue microarrays from 13 PDTC and 35 advanced PTC patients. VEGF-A expression in both cancer cells and vasculature coincided with CD31- or ERG-positive areas (Fig. 5A–C), whereas CXCL8 was dominantly expressed in cancer cells (Fig. 5D). CD163-positive macrophages were observed at stromal sites (Fig. 5E). In PDTC samples, VEGF-A expression showed positive correlations with CD31 (Fig. 5F), ERG (Fig. 5G), CD163 (Fig. 5H), and CXCL8 expression (Fig. 5I), although the correlation with ERG was marginally significant ($r = 0.507$, $P = 0.077$, Fig. 5G). Consistent to the PDTC data, 35 advanced PTC patients with a tumor size of ≥ 2 cm also showed that the VEGF-A expression showed positive correlations with CD163 and CXCL8 expressions (Supplementary Table S2).

Next, the clinical characteristics of PDTC patients according to preoperative serum TSH levels and VEGF-A expression were analyzed. Preoperative serum TSH levels were positively related with VEGF-A expression ($r = 0.583$, $P = 0.036$, Fig. 5J) and larger tumor size ($r = 0.677$, $P = 0.011$, Fig. 5K), but not significantly associated with CD31 ($r = 0.183$, $P = 0.550$). Tumor size also positively associated with VEGF-A expression ($r = 0.526$, $P = 0.065$, Fig. 5L). Interestingly, patients with higher VEGF-A expression showed significantly higher rates of distant metastasis and poor disease specific survivals (Table 1 and Fig. 5M).

Discussion

The present study demonstrated that TSH stimulated secretion of angiogenic factors such as VEGF-A and CXCL8 in PDTC cells, which showed TSH/cAMP-independent cell growth, through TSH/AKT and ERK pathways. As a result, TSH-stimulated tumor angiogenesis enhanced tumor growth in association with enhanced macrophage infiltration. Because treatment

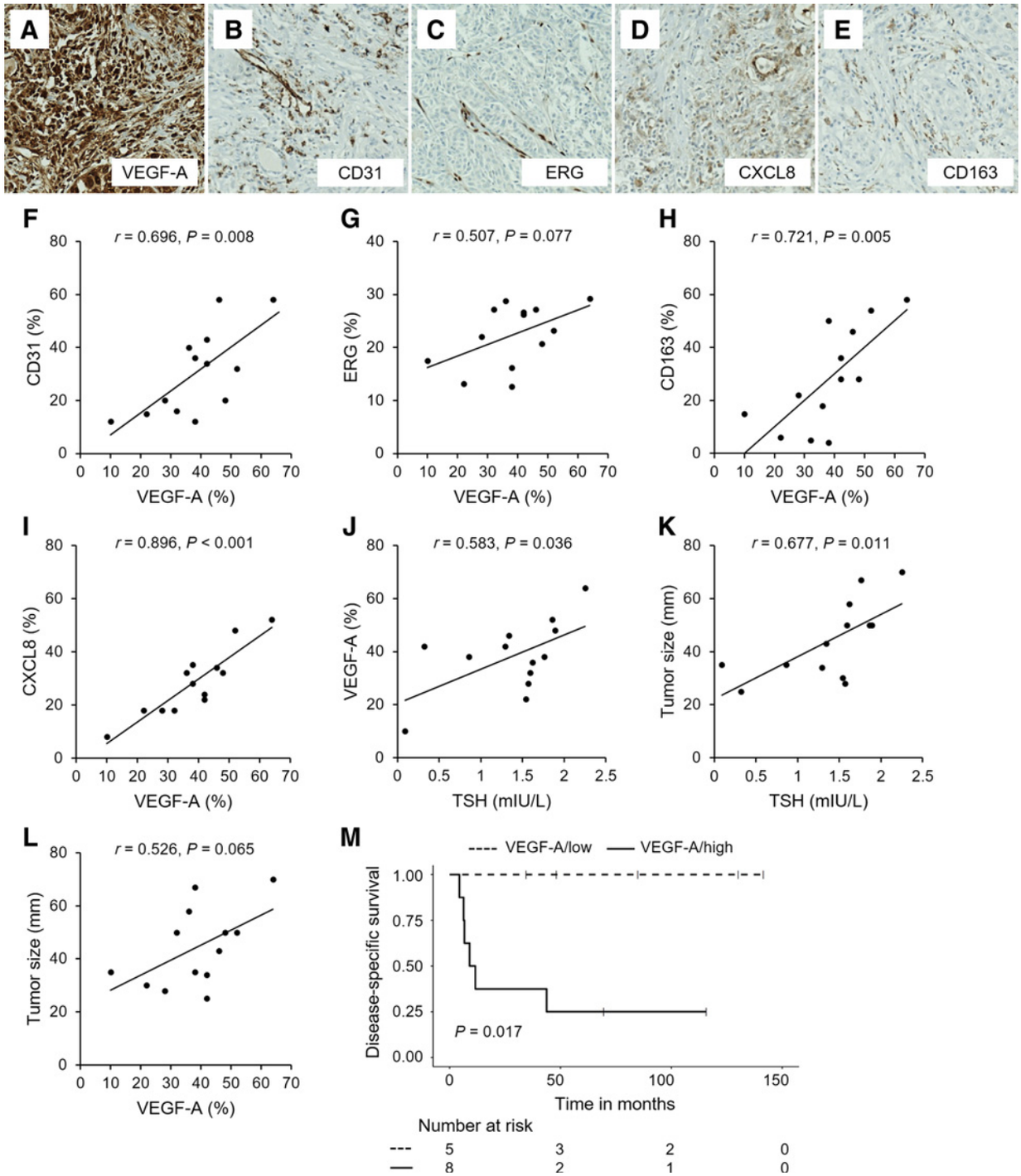

Figure 5.

Associations of VEGF-A with tumor angiogenesis, macrophage infiltration, and CXCL8 expression and associations among serum TSH levels, VEGF-A, and tumor size in human PDTC. IHC staining using anti–VEGF-A, anti-CD31, anti-ERG, anti-CXCL8, and anti-CD163 antibodies was performed on tissue microarrays of human PDTC ($n = 13$). Representative images of (**A**) VEGF-A, (**B**) CD31, (**C**) ERG, (**D**) CXCL8, and (**E**) CD163 from the same subject (×100; arrows, intratumoral vasculature). The immunoactivity of all stains was analyzed using the Immunoratio or ImageScope software. The correlations between (**F**) VEGF-A and CD31, (**G**) VEGF-A and ERG, (**H**) VEGF-A and CD163, and (**I**) VEGF-A and CXCL8 are illustrated. Correlations between (**J**) preoperative serum TSH levels and the immunoactivity of VEGF-A, (**K**) preoperative serum TSH levels and tumor size, and (**L**) the immunoactivity of VEGF-A and tumor size are illustrated. $r =$ the Pearson correlation coefficient. **M,** Disease-specific survival for patients with PDTC. Based on the median value (38%) of immunoactivity scores of VEGF-A, the value lower than this was classified as VEGF-A/low, and the value equal to or higher than this was classified as VEGF-A/high.

Table 1. Clinicopathologic characteristics of patients with PDTC according to VEGF-A expression

	VEGF-A ($n = 13$)		
	Low	**High**	***P***
Cases	5	8	
Age at diagnosis[a]	49.0 (34.0–67.5)	64.5 (59.5–78.8)	0.213
Male sex, *n* (%)	1 (20.0)	4 (50.0)	0.565
Serum TSH, preoperative (μIU/L)[a]	1.6 (0.8–1.6)	1.6 (1.0–1.9)	0.622
Tumor size (mm^3)[a]	35.0 (29.0–54.0)	46.5 (34.3–62.8)	0.524
Lymph node metastasis, *n* (%)	3 (60.0)	7 (87.5)	0.510
Distant metastasis, *n* (%)	0 (0.0)	7 (87.5)	0.005
Persistence, *n* (%)	0 (0.0)	6 (75.0)	0.021
Death of disease, *n* (%)	0 (0.0)	6 (75.0)	0.021
Disease-specific survival, months[a]	84.8 (41.3–135.7)	10.3 (6.4–63.0)	0.045

NOTE: Based on the median value (38%) of VEGF-A expression, the value lower than this was classified as low and the value equal to or higher than this was classified as high.

[a]Values presented as median (interquartile range) and *P* values by Mann–Whitney *U* test.

of neutralizing antibodies blocking VEGF and/or CXCL8 or macrophage inhibitor reduced TSH-dependent tumor growth *in vivo*, we concluded that TSH-mediated tumor angiogenesis is essential for tumor growth of PDTCs. In human thyroid cancer tissue microarrays, preoperative levels of TSH were positively correlated with VEGF-A and tumor size, and the expression of VEGF-A was positively correlated with CD31, CD163, and CXCL8, as well as their clinical poor prognosis, suggesting that TSH might affect tumor progression by modulating tumor angiogenesis and microenvironments in PDTCs. Taken together, the present study supports the usefulness of T4 suppression therapy, even in PDTCs that lose some characteristics of differentiated cells, and thus do not show TSH-dependent growth.

Classically, TSH has been established to play a role in tumor cell growth through receptor signaling, especially at the time of thyroid cancer initiation (17). However, during cancer progression, *TSHR* is silenced in some tumor cells, and the differentiation status of each tumor cell becomes heterogeneous. In this stage, it is reasonable to assume that T4 suppression therapy no longer exerts effects on controlling cancer cell growth (33). However, TSH also modulates the transcription of several genes in these cells (19–21). The present study clearly demonstrated that TSH stimulated angiogenic cytokines, including VEGF-A and CXCL8, in a PDTC cell line, with minimal expression of *TSHR*. In the context of the alternative role of TSH signaling in gene transcription, T4 suppression therapy could still be beneficial in PDTCs, even those in which the expression of *TSHR* is very low, because T4 suppression therapy would help control the tumor microenvironment. The next question would be the cutoff value of TSH for these proangiogenic actions. The present study did not show dose-dependent response of TSH on tumor growth, although there were positive correlations between the serum TSH levels and CD31 expressions. Further studies with human-relevant model are needed to explore the protumorigenic threshold of TSH.

Growing evidence indicates that TSH has biological functions in various human cells other than thyrocytes, such as fibroblasts (23), immune cells (34), and endothelial cells (22). Moreover, a recent study suggested that TSH may directly stimulate endothelial cells and promote angiogenesis (22). Based on this evidence, one of the specific aims of this study was to investigate whether TSH has direct effects on endothelial cells and contributes to the enhancement of tumor angiogenesis *in vivo* or not. If the effects of TSH on endothelial cells in the tumor microenvironment are sufficiently strong to modulate tumor vasculature, TSH signaling might have a role in the tumor microenvironment of other human cancers. Elevated serum TSH, whether overt or due to subclinical hypothyroidism, is a common human pathology in the general population (35), especially in cancer patients as it relates to antithyroid treatment (36). However, the present study, using an ectopic tumor model of breast cancer cells, demonstrated that the preangiogenic effects of TSH on human cancers without TSHR expression were limited, but further studies using various human cancer cell lines other than breast cancer cells are needed to validate it.

An interesting finding of this study is that thyroid cancer cells that showed TSH/cAMP-independent growth still responded to TSH stimulation and changed their gene transcriptional activities. Although Gsα–cAMP signaling is the canonical pathway known to regulate the proliferation and differentiation of thyrocytes, the existence of other aberrant pathways, such as PI3K/AKT and PKC/ERK, and their signaling cross-talk has been intensively studied using various TSH receptor antibodies (31). Moreover, previous studies have shown that TSH regulated IL6 or secretory IL1 receptor antagonist production in fibrocytes through the PI3K/AKT pathway, independently of Gsα–cAMP signaling (37, 38). Here, we demonstrated that TSH alternatively activated the PI3K/AKT and ERK pathways, and subsequently regulated *VEGF-A* and *CXCL8* transcription in thyroid cancer cells showing minimal *TSHR* expression. These data suggest that even in cancer cells that show limited expression of *TSHR* and lose their differentiation status, TSH can still affect the transcriptional activities of many genes, promoting tumor angiogenesis and growth by activating aberrant TSH signaling. One of the possible explanations for the effects of TSH on thyroid cancer cells that minimally express *TSHR* is that gain-of-function mutations could be involved (33, 39), although further studies are needed to clarify this.

In the present study, TSH increased CXCL8 secretion in conjunction with VEGF-A. Previously, several studies have demonstrated that TSH or tumor necrosis factor-α stimulated CXCL8 production in normal thyrocytes, playing a role in the immune process in thyroiditis (21, 40). In the thyroid cancer microenvironment, CXCL8, originating from mast cells or macrophages (41, 42), has been established as an angiogenic cytokine that modulates tumor vasculature (41, 43). Herein, we first demonstrated that TSH upregulated CXCL8 production in thyroid cancer cells. Furthermore, in microvascular endothelial cells, simultaneous inhibition of VEGF-A and CXCL8 using neutralizing antibodies blocked tube formation potential in a synergistic manner, suggesting a possible biological relevance of VEGF-A and CXCL8. A previous study demonstrated that

CXCL8 stimulated VEGF-A production and reinforced an autocrine loop in VEGF-A/VEGF receptor 2 signaling in murine endothelial cells (44). Taken together, CXCL8 might support VEGF-A action in thyroid cancer microenvironments (Fig. 4C).

The associations among TSH, VEGF-A, and CXCL8 were validated in human PDTC tissues alongside an assessment of the density of endothelial cells and macrophages in tumor microenvironments. The sample size was small, still preoperative TSH levels were positively correlated with VEGF-A expression and tumor size, and finally VEGF-A was associated with poor clinical outcomes including poor disease-specific survival. Meanwhile, although VEGF-A expression was positively correlated with CD31, preoperative TSH levels were not correlated with CD31, suggesting that TSH might indirectly affect tumor angiogenesis. Several angiogenic factors including VEGF-A and CXCL8 or other cellular responses might mediate the link between TSH and tumor angiogenesis. Further human study with large sample size is needed to clarify it.

In conclusion, TSH signaling modulated tumor angiogenesis and macrophage infiltration, and enhanced tumor growth by stimulating VEGF-A and CXCL8 secretions from thyroid cancer cells. Higher preoperative TSH levels were associated with the higher expression of VEGF-A, which was related to higher vascular density, macrophage infiltration, and poor prognosis. Given these aberrant actions of TSH signaling on thyroid cancer cells, T4 suppression therapy might be beneficial not only in well-differentiated cancers that show TSH-dependent growth, but also in PDTCs.

Disclosure of Potential Conflicts of Interest

No potential conflicts of interest were disclosed.

Authors' Contributions

Conception and design: Y.S. Song, S.W. Cho, Y.J. Park
Development of methodology: Y.S. Song, S.W. Cho, Y.J. Park
Acquisition of data (provided animals, acquired and managed patients, provided facilities, etc.): S.W. Cho, Y.J. Park
Analysis and interpretation of data (e.g., statistical analysis, biostatistics, computational analysis): Y.S. Song, S.W. Cho
Writing, review, and/or revision of the manuscript: Y.S. Song, M.J. Kim, H.J. Sun, H.H. Kim, H.S. Shin, Y.A. Kim, B.-C. Oh, S.W. Cho, Y.J. Park
Administrative, technical, or material support (i.e., reporting or organizing data, constructing databases): Y.S. Song, M.J. Kim, H.J. Sun, H.H. Kim, H.S. Shin, Y.A. Kim, B.-C. Oh, S.W. Cho
Study supervision: S.W. Cho, Y.J. Park

Acknowledgments

This work was supported by a grant of the Korea Health Technology R&D Project through the Korea Health Industry Development Institute (KHIDI, HI14C1277), and a grant from the National R&D Program for Cancer Control (HA17C0040) funded by the Ministry of Health and Welfare, Republic of Korea and by the Basic Science Research Program through the National Research Foundation of Korea (NRF) funded by the Ministry of Science, ICT and Future Planning (2013R1A1A3007152).

The costs of publication of this article were defrayed in part by the payment of page charges. This article must therefore be hereby marked *advertisement* in accordance with 18 U.S.C. Section 1734 solely to indicate this fact.

Received February 27, 2018; revised July 20, 2018; accepted October 9, 2018; published first October 12, 2018.

References

1. Howlader N, Noone AM, Krapcho M, Miller D, Bishop K, Altekruse SF, et al. SEER cancer statistics review, 1975-2013, Bethesda, MD:National Cancer Institute. Available from: http://seer.cancer.gov/csr/1975_2013/, based on November 2016 SEER data submission, posted to the SEER web site, April 2017.
2. Cho BY, Choi HS, Park YJ, Lim JA, Ahn HY, Lee EK, et al. Changes in the clinicopathological characteristics and outcomes of thyroid cancer in Korea over the past four decades. Thyroid 2013;23:797–804.
3. Magarey MJ, Freeman JL. Recurrent well-differentiated thyroid carcinoma. Oral Oncol 2013;49:689–94.
4. Haugen BR, Alexander EK, Bible KC, Doherty GM, Mandel SJ, Nikiforov YE, et al. 2015 American thyroid association management guidelines for adult patients with thyroid nodules and differentiated thyroid cancer: the American Thyroid Association Guidelines Task Force on thyroid nodules and differentiated thyroid cancer. Thyroid 2016;26:1–133.
5. Yi KH, Lee EK, Kang HC, Koh Y, Kim SW, Kim IJ, et al. 2016 revised Korean Thyroid Association Management guidelines for patients with thyroid nodules and thyroid cancer. Int J Thyroidol 2016;9:59–126.
6. Pacini F, Schlumberger M, Dralle H, Elisei R, Smit JW, Wiersinga W, et al. European consensus for the management of patients with differentiated thyroid carcinoma of the follicular epithelium. Eur J Endocrinol 2006;154:787–803.
7. Sundram F, Robinson BG, Kung A, Lim-Abrahan MA, Bay NQ, Chuan LK, et al. Well-differentiated epithelial thyroid cancer management in the Asia Pacific region: a report and clinical practice guideline. Thyroid 2006;16:461–9.
8. Fiore E, Rago T, Provenzale MA, Scutari M, Ugolini C, Basolo F, et al. Lower levels of TSH are associated with a lower risk of papillary thyroid cancer in patients with thyroid nodular disease: thyroid autonomy may play a protective role. Endocr Relat Cancer 2009;16:1251–60.
9. Haymart MR, Repplinger DJ, Leverson GE, Elson DF, Sippel RS, Jaume JC, et al. Higher serum thyroid stimulating hormone level in thyroid nodule patients is associated with greater risks of differentiated thyroid cancer and advanced tumor stage. J Clin Endocrinol Metab 2008;93:809–14.
10. Tam AA, Ozdemir D, Aydin C, Bestepe N, Ulusoy S, Sungu N, et al. Association between preoperative thyrotrophin and clinicopathological and aggressive features of papillary thyroid cancer. Endocrine 2018;59:565–72.
11. Hovens GC, Stokkel MP, Kievit J, Corssmit EP, Pereira AM, Romijn JA, et al. Associations of serum thyrotropin concentrations with recurrence and death in differentiated thyroid cancer. J Clin Endocrinol Metab 2007;92:2610–5.
12. Jonklaas J, Sarlis NJ, Litofsky D, Ain KB, Bigos ST, Brierley JD, et al. Outcomes of patients with differentiated thyroid carcinoma following initial therapy. Thyroid 2006;16:1229–42.
13. Sawin CT, Geller A, Wolf PA, Belanger AJ, Baker E, Bacharach P, et al. Low serum thyrotropin concentrations as a risk factor for atrial fibrillation in older persons. N Engl J Med 1994;331:1249–52.
14. Uzzan B, Campos J, Cucherat M, Nony P, Boissel JP, Perret GY. Effects on bone mass of long term treatment with thyroid hormones: a meta-analysis. J Clin Endocrinol Metab 1996;81:4278–89.
15. Moon JH, Jung KY, Kim KM, Choi SH, Lim S, Park YJ, et al. The effect of thyroid stimulating hormone suppressive therapy on bone geometry in the hip area of patients with differentiated thyroid carcinoma. Bone 2016;83:104–10.
16. Lazar V, Bidart JM, Caillou B, Mahe C, Lacroix L, Filetti S, et al. Expression of the Na+/I- symporter gene in human thyroid tumors: a comparison study with other thyroid-specific genes. J Clin Endocrinol Metab 1999;84:3228–34.
17. Kimura T, Van Keymeulen A, Golstein J, Fusco A, Dumont JE, Roger PP. Regulation of thyroid cell proliferation by TSH and other factors: a critical evaluation of in vitro models. Endocr Rev 2001;22:631–56.
18. Saito T, Endo T, Kawaguchi A, Ikeda M, Nakazato M, Kogai T, et al. Increased expression of the Na+/I- symporter in cultured human thyroid cells exposed to thyrotropin and in Graves' thyroid tissue. J Clin Endocrinol Metab 1997;82:3331–6.
19. Fiore L, Pollina LE, Fontanini G, Casalone R, Berlingieri MT, Giannini R, et al. Cytokine production by a new undifferentiated human

thyroid carcinoma cell line, FB-1. J Clin Endocrinol Metab 1997; 82:4094–100.
20. Hoffmann S, Hofbauer LC, Scharrenbach V, Wunderlich A, Hassan I, Lingelbach S, et al. Thyrotropin (TSH)-induced production of vascular endothelial growth factor in thyroid cancer cells in vitro: evaluation of TSH signal transduction and of angiogenesis-stimulating growth factors. J Clin Endocrinol Metab 2004;89:6139–45.
21. Watson PF, Pickerill AP, Davies R, Weetman AP. Semi-quantitative analysis of interleukin-1 alpha, interleukin-6 and interleukin-8 mRNA expression by human thyrocytes. J Mol Endocrinol 1995;15:11–21.
22. Balzan S, Del Carratore R, Nicolini G, Beffy P, Lubrano V, Forini F, et al. Proangiogenic effect of TSH in human microvascular endothelial cells through its membrane receptor. J Clin Endocrinol Metab 2012;97: 1763–70.
23. Agretti P, De Marco G, De Servi M, Marcocci C, Vitti P, Pinchera A, et al. Evidence for protein and mRNA TSHr expression in fibroblasts from patients with thyroid-associated ophthalmopathy (TAO) after adipocytic differentiation. Eur J Endocrinol 2005;152:777–84.
24. Ahn SH, Henderson Y, Kang Y, Chattopadhyay C, Holton P, Wang M, et al. An orthotopic model of papillary thyroid carcinoma in athymic nude mice. Arch Otolaryngol Head Neck Surg 2008;134:190–7.
25. Colzani RM, Alex S, Fang SL, Braverman LE, Emerson CH. The effect of recombinant human thyrotropin (rhTSH) on thyroid function in mice and rats. Thyroid 1998;8:797–801.
26. Tomayko MM, Reynolds CP. Determination of subcutaneous tumor size in athymic (nude) mice. Cancer Chemother Pharmacol 1989;24: 148–54.
27. Cho SW, Kim YA, Sun HJ, Kim YA, Oh BC, Yi KH, et al. CXCL16 signaling mediated macrophage effects on tumor invasion of papillary thyroid carcinoma. Endocr Relat Cancer 2016;23:113–24.
28. Schneider CA, Rasband WS, Eliceiri KW. NIH image to ImageJ: 25 years of image analysis. Nat Methods 2012;9:671–5.
29. Tuominen VJ, Ruotoistenmaki S, Viitanen A, Jumppanen M, Isola J. ImmunoRatio: a publicly available web application for quantitative image analysis of estrogen receptor (ER), progesterone receptor (PR), and Ki-67. Breast Cancer Res 2010;12:R56.
30. Schweppe RE, Klopper JP, Korch C, Pugazhenthi U, Benezra M, Knauf JA, et al. Deoxyribonucleic acid profiling analysis of 40 human thyroid cancer cell lines reveals cross-contamination resulting in cell line redundancy and misidentification. J Clin Endocrinol Metab 2008; 93:4331–41.
31. Morshed SA, Latif R, Davies TF. Characterization of thyrotropin receptor antibody-induced signaling cascades. Endocrinology 2009;150:519–29.
32. Kim S, Cho SW, Min HS, Kim KM, Yeom GJ, Kim EY, et al. The expression of tumor-associated macrophages in papillary thyroid carcinoma. Endocrinol Metab (Seoul) 2013;28:192–8.
33. Garcia-Jimenez C, Santisteban P. TSH signalling and cancer. Arq Bras Endocrinol Metabol 2007;51:654–71.
34. Bagriacik EU, Klein JR. The thyrotropin (thyroid-stimulating hormone) receptor is expressed on murine dendritic cells and on a subset of CD45RBhigh lymph node T cells: functional role for thyroid-stimulating hormone during immune activation. J Immunol 2000;164: 6158–65.
35. Roberts CG, Ladenson PW. Hypothyroidism. Lancet 2004;363:793–803.
36. Kurtin SE. Hypothyroidism: a growing complication of cancer treatment. Oncology 2009;23:41–5.
37. Li B, Smith TJ. PI3K/AKT pathway mediates induction of IL-1RA by TSH in fibrocytes: modulation by PTEN. J Clin Endocrinol Metab 2014;99: 3363–72.
38. Raychaudhuri N, Fernando R, Smith TJ. Thyrotropin regulates IL-6 expression in CD34+ fibrocytes: clear delineation of its cAMP-independent actions. PLoS One 2013;8:e75100.
39. Russo D, Arturi F, Schlumberger M, Caillou B, Monier R, Filetti S, et al. Activating mutations of the TSH receptor in differentiated thyroid carcinomas. Oncogene 1995;11:1907–11.
40. Rotondi M, Coperchini F, Pignatti P, Sideri R, Groppelli G, Leporati P, et al. Interferon-gamma and tumor necrosis factor-alpha sustain secretion of specific CXC chemokines in human thyrocytes: a first step toward a differentiation between autoimmune and tumor-related inflammation? J Clin Endocrinol Metab 2013;98:308–13.
41. Visciano C, Liotti F, Prevete N, Cali G, Franco R, Collina F, et al. Mast cells induce epithelial-to-mesenchymal transition and stem cell features in human thyroid cancer cells through an IL-8-Akt-Slug pathway. Oncogene 2015;34:5175–86.
42. Fang W, Ye L, Shen L, Cai J, Huang F, Wei Q, et al. Tumor-associated macrophages promote the metastatic potential of thyroid papillary cancer by releasing CXCL8. Carcinogenesis 2014;35:1780–7.
43. Passaro C, Borriello F, Vastolo V, Di Somma S, Scamardella E, Gigantino V, et al. The oncolytic virus dl922–947 reduces IL-8/CXCL8 and MCP-1/CCL2 expression and impairs angiogenesis and macrophage infiltration in anaplastic thyroid carcinoma. Oncotarget 2016;7:1500–15.
44. Martin D, Galisteo R, Gutkind JS. CXCL8/IL8 stimulates vascular endothelial growth factor (VEGF) expression and the autocrine activation of VEGFR2 in endothelial cells by activating NFkappaB through the CBM (Carma3/Bcl10/Malt1) complex. J Biol Chem 2009;284: 6038–42.